

AD-A209 490

DTIC FILE COPY

2

OFFICE OF NAVAL RESEARCH
Research Contract N00014-87-K-0014
R&T Code 413a001

Technical Report No. 18

INITIAL STAGES OF METAL/SEMICONDUCTOR INTERFACE FORMATION:
Au AND Ag ON Si(111)

by

R. Stanley Williams, Richard S. Daley, Judy H. Huang,
and Robert M. Charatan

To be published
in
Applications of Surface Science

SDTIC
ELECTE
JUN 22 1989
H

University of California, Los Angeles
Department of Chemistry & Biochemistry and Solid State Science Center
Los Angeles, CA 90024-1569

July 1, 1989

Reproduction in whole or part is permitted for any purpose of the United States Government.

This document has been approved for public release and sale;
its distribution is unlimited

89 6 21 024

UNCLASSIFIED

SECURITY CLASSIFICATION OF THIS PAGE

REPORT DOCUMENTATION PAGE

1a. REPORT SECURITY CLASSIFICATION UNCLASSIFIED		1b. RESTRICTIVE MARKINGS N/A	
2a. SECURITY CLASSIFICATION AUTHORITY N/A		3. DISTRIBUTION/AVAILABILITY OF REPORT Approved for public release; distribution unlimited	
2b. DECLASSIFICATION/DOWNGRADING SCHEDULE N/A			
4. PERFORMING ORGANIZATION REPORT NUMBER(S) N/A		5. MONITORING ORGANIZATION REPORT NUMBER(S)	
6a. NAME OF PERFORMING ORGANIZATION The Regents of the University of California	6b. OFFICE SYMBOL (if applicable)	7a. NAME OF MONITORING ORGANIZATION 1) ONR Pasadena - Administrative 2) ONR Alexandria - Technical	
6c. ADDRESS (City, State, and ZIP Code) Office of Contracts & Grants Administration U C L A, 405 Hilgard Avenue Los Angeles, CA 90024		7b. ADDRESS (City, State, and ZIP Code) 1) 1030 E. Green Street, Pasadena, CA 91106 2) 800 N. Quincy St., Arlington, VA 22217-5000	
8a. NAME OF FUNDING/SPONSORING ORGANIZATION Office of Naval Research	8b. OFFICE SYMBOL (if applicable) ONR	9. PROCUREMENT INSTRUMENT IDENTIFICATION NUMBER N00014-87-K-0014	
8c. ADDRESS (City, State, and ZIP Code) 800 N. Quincy Street, 614A:DHP Arlington, VA 22217-5000		10. SOURCE OF FUNDING NUMBERS	
		PROGRAM ELEMENT NO.	PROJECT NO.
		TASK NO.	WORK UNIT ACCESSION NO.
11. TITLE (Include Security Classification) UNCLASSIFIED: Initial stages of metal/semiconductor interface formation: Au and Ag on Si(111)			
12. PERSONAL AUTHOR(S) R. Stanley Williams, Richard S. Daley, Judy H. Huang and Robert M. Charatan			
13a. TYPE OF REPORT Tech. Rept. #18	13b. TIME COVERED FROM 1988 TO 1989	14. DATE OF REPORT (Year, Month, Day) 20 June 1989	15. PAGE COUNT 14
16. SUPPLEMENTARY NOTATION			
17. COSATI CODES		18. SUBJECT TERMS (Continue on reverse if necessary and identify by block number) atomic structure - monolayer coverage - ICISS - hollow sites - trimer vs. honeycomb structures - interatomic distance	
FIELD	GROUP SUB-GROUP		
19. ABSTRACT (Continue on reverse if necessary and identify by block number) We have studied the atomic structures formed by monolayer coverages of Au and Ag on the Si(111) surface using primarily the technique of the Impact-Collision Ion Scattering Spectroscopy (ICISS). For the case of Au films annealed at 700°C, three different types of LEED patterns are formed depending on the fractional monolayer coverage: 5x1, $\sqrt{3} \times \sqrt{3}$, and 6x6. The ICISS data reveal that all the three surfaces are structurally similar: the Au atoms reside above the Si(111) plane, most likely in threefold-hollow sites, and the different surfaces appear to be characterized by rows (5x1) or a honeycomb network ($\sqrt{3} \times \sqrt{3}$ and 6x6). In contrast, the Ag films deposited at elevated substrate temperature (480°C) display only a $\sqrt{3} \times \sqrt{3}$ LEED pattern for coverages ranging from 0.25 to 35 monolayers. A trimer model appears to be more consistent with the low-coverage Ag ICISS data rather than a honeycomb arrangement of the Ag atoms.			
20. DISTRIBUTION/AVAILABILITY OF ABSTRACT <input checked="" type="checkbox"/> UNCLASSIFIED/UNLIMITED <input type="checkbox"/> SAME AS RPT <input type="checkbox"/> DTIC USERS		21. ABSTRACT SECURITY CLASSIFICATION UNCLASSIFIED	
22a. NAME OF RESPONSIBLE INDIVIDUAL R. Stanley Williams		22b. TELEPHONE (Include Area Code) (213) 825-8818	22c. OFFICE SYMBOL UCLA

Initial Stages of Metal/Semiconductor Interface Formation:
Au and Ag on Si(111)

R. Stanley Williams, Richard S. Daley, Judy H. Huang, and Robert M. Charatan

Department of Chemistry & Biochemistry
and Solid State Science Center
University of California Los Angeles
Los Angeles, CA 90024-1569

Abstract

We have studied the atomic structures formed by monolayer coverages of Au and Ag on the Si(111) surface using primarily the technique of Impact-Collision Ion Scattering Spectroscopy (ICISS). For the case of Au films annealed at 700° C, three different types of LEED patterns are formed depending on the fractional monolayer coverage: 5x1, $\sqrt{3}\times\sqrt{3}$, and 6x6. The ICISS data reveal that all the three surfaces are structurally similar: the Au atoms reside above the Si(111) plane, most likely in threefold-hollow sites, and the different surfaces appear to be characterized by rows (5x1) or a honeycomb network ($\sqrt{3}\times\sqrt{3}$ and 6x6). In contrast, the Ag films deposited at elevated substrate temperature (480° C) display only a $\sqrt{3}\times\sqrt{3}$ LEED pattern for coverages ranging from 0.25 to 35 monolayers. A trimer model appears to be more consistent with the low coverage Ag ICISS data rather than a honeycomb arrangement of the Ag atoms.

1. Introduction

The reconstructions induced on the Si(111) surface by the noble metals Au and Ag have been the subjects of many scientific investigations for a great many years [1,2], but as yet there is no consensus on their detailed atomic structures. If anything, the number of proposed structural models has increased in proportion to the number of studies. This is principally because each of the currently utilized surface structure techniques is sensitive to a different aspect of the surface structure. One might think that the most direct real-space technique, Scanning Tunneling Microscopy (STM), would resolve any ambiguities. However, as demonstrated last year by two consecutive papers in Physical Review Letters on the Ag-induced $\sqrt{3}\times\sqrt{3}$ Si(111) surface [3,4], STM is not yet capable of elemental recognition. Although both papers showed essentially identical honeycomb patterns, one group concluded that the STM features were caused by Si adatoms atop Ag trimers [3] and the other decided that the STM features were individual Ag adatoms [4]. A recent X-ray diffraction study concluded that this surface was characterized by Ag trimers, but without Si adatoms above the trimers [5]. An STM study of a surface that might be structurally similar, that is the Au-induced $\sqrt{3}\times\sqrt{3}$ Si(111) surface, revealed triangular shaped features that were interpreted to be Au trimers [6], although later work showed the features to be essentially circular [7]. Our previous Impact-Collision Ion Scattering Spectroscopy (ICISS) [8] studies of Au: $\sqrt{3}\times\sqrt{3}$ Si(111) were shown to be consistent with a honeycomb structure [9].

Ion scattering techniques do not directly image a surface, but they do have several advantages for structural analysis: the data provide real-space information (*i.e.* no diffraction), the scattering features are determined by the nuclear positions (not the valence electrons), and the scattered-ion energy depends on the mass of the scattering atom (elemental specificity). In this paper, we will review the bases of our conclusions regarding the structure of the Au-induced Si(111) reconstructions and argue that a honeycomb model is consistent with the published STM images [6]. We also present ICISS data for the Ag-induced $\sqrt{3}\times\sqrt{3}$ Si(111) surface, and conclude that the local atomic structures of the Au- and Ag-covered Si(111) surfaces are probably different.



Availability Codes	
Dist	Avail and/or Special
A-1	

The ICISS data from the Ag covered surface is more consistent with a trimer arrangement [5] than a honeycomb, but the latter cannot be strictly ruled out based on our data alone.

II. Experimental Procedure

The substrates used in this study were mirror-smooth Si(111) wafers measuring 1.5x0.7 cm. The surfaces were prepared by resistively heating the samples in an ultra-high vacuum chamber to alternately anneal and flash them to 1050° C until sharp 7x7 LEED patterns were observed. No surface contaminants could be detected by Auger spectroscopy. The noble metal films were deposited by evaporating either Au or Ag from a tungsten filament onto a room temperature substrate and then annealing to 700° C (Au) or onto a substrate maintained at 480° C (Ag). The deposition thickness in monolayers (ML) was monitored with a quartz crystal oscillator. The Au films were much more stable than the Ag films, since the Au could not be removed by heating, but the Ag could be completely removed to recover a clean 7x7 surface by annealing to 800° C.

The ICISS experiments were performed as described previously [9,10] using 5 keV Li ions as projectiles and a constant scattering angle of 157° (Au) or 155° (Ag). No ion-bombardment damage was observed for the Li ion dose required to accumulate an ICISS scan from the Au-covered surfaces, but some systematic reduction of the scattering intensity did occur for the Ag-covered surfaces.

III. Results and Discussion

The ICISS data for scattering from the Au adatoms of the three Au-covered surfaces that produced the sharpest LEED spots (and thus presumably the most well ordered reconstructions) are shown in Fig. 1 for the 5x1 (0.4 ML), $\sqrt{3}\times\sqrt{3}$ (0.8 ML), and 6x6 (1.1 ML) reconstructions. The data for the different surfaces are all similar, which implies that the local atomic structures of the three reconstructions are similar. Each ICISS scan reveals an intense surface flux peak, with no intensity modulations at higher polar angles. This is firm evidence that for all three surfaces the Au atoms reside above the outermost Si plane, for otherwise there should be orientations at which Si could block incident Li ions from hitting Au atoms and cause a local minimum in the

scattering yield. The ICISS data along the four major azimuths in the Si(111) plane, that is the $[1\bar{1}0]$, $[\bar{1}10]$, $[11\bar{2}]$, and $[\bar{1}\bar{1}2]$, are consistent with the only model so far proposed for the 5×1 surface [1], as reported previously [10], so this reconstruction will not be discussed further.

For the cases of the $\sqrt{3}\times\sqrt{3}$ and 6×6 reconstructions, many variations of all the previously proposed models have been investigated [9] by comparing the experimentally determined ICISS angular distributions to computer simulations [11]. The models most consistent with the experimental data were the honeycomb model shown in Fig. 2a for the $\sqrt{3}\times\sqrt{3}$ surface and the centered-hexagon structure (a honeycomb with an additional Au atom in the center of each hexagon but displaced vertically downward from the honeycomb plane by 0.3 \AA) for the 6×6 surface. Calculated ICISS distributions for these models are shown as dashed lines in Fig. 1. Although the agreement between the model calculations and the experimental data was reasonable, it could be improved, as shown by the solid lines of Fig. 1, by considering each surface to be a combination of both the honeycomb and centered-hexagon structures. Such a model is reasonable for the $\sqrt{3}\times\sqrt{3}$ surface, since an ideal honeycomb structure would consist of 0.67 ML Au , whereas the experimentally determined Au coverage was 0.8 ML . Placing the equivalent of 0.13 ML of Au atoms in the centers of the hexagons and displacing them downward 0.3 \AA significantly improved the agreement between the calculated and experimental ICISS scans. In the case of the 6×6 structure, the agreement between the experimental data and the simulations for the centered-hexagon model was improved by removing the equivalent of 25% of the Au atoms from the centers of the hexagons. An arrangement of centered- and empty-hexagons that would produce a 6×6 LEED pattern is shown in Fig. 2b. Therefore, the experimentally observed Si(111) surface with Au coverages greater than 0.4 ML is probably always a mixture of honeycomb and centered-hexagon subunits (both give rise to a $\sqrt{3}\times\sqrt{3}$ unit cell), since it is likely that the difference in adsorption energy between the two reconstructions is small [12]. At higher coverages, long range order in the arrangement of the empty hexagons, reminiscent of the 7×7 structure of the clean Si surface, produces the 6×6 structure. The fact that the STM images of this surface did not show a honeycomb pattern [6] may be the result of the inability of the STM to resolve Au-atom pairs

along the $\langle 110 \rangle$ azimuths (the short Au-Au distance in the honeycomb). Analysis of 5 keV Li scattered from Si atoms for the $\sqrt{3} \times \sqrt{3}$ and 6×6 structures [9] shows the threefold-hollow site to be preferred over the threefold-atop for Au adsorption.

The ICISS data for 5 keV Li ions scattered from Ag atoms of the Ag-induced Si(111) $\sqrt{3} \times \sqrt{3}$ surface looks considerably different from that for the corresponding Au-covered surface along the $[\bar{1}10]$ azimuth, but data along the $[11\bar{2}]$ azimuth is similar, as shown in Fig. 3 for a 0.25 ML coverage of Ag. For higher coverages (≥ 1.0 ML) the flux peaks along both azimuths begin to broaden; the additional scattering trajectories may arise because of the initiation of Ag island formation [1]. The surface flux peak for the Ag-induced $\sqrt{3} \times \sqrt{3}$ surface along the $[\bar{1}10]$ azimuth is considerably narrower and does not have the pronounced shoulder seen for the Au-induced reconstruction. Indeed, the Ag $[\bar{1}10]$ ICISS angular distribution is similar to that calculated previously for a Au-trimer model [9]. In addition, the progression in LEED patterns as a function of coverage from 5×1 through $\sqrt{3} \times \sqrt{3}$ to 6×6 observed for the Au:Si(111) surfaces were not present in the Ag:Si(111) system. All Ag coverages from 0.25 to 35 ML exhibited a $\sqrt{3} \times \sqrt{3}$ LEED pattern. Also, the Ag-covered Si surface was much more sensitive to ion-bombardment and heating than the Au-covered surface.

These observations are evidence that the atomic structures of the Au- and Ag-induced $\sqrt{3} \times \sqrt{3}$ reconstructions of Si(111) are structurally different. Figure 3 shows calculations that have been least squares fit to the data for the honeycomb model and the trimer model of Fig. 4, which is based on the chemically intuitive bonding arrangement shown in the inset. This set of Ag ICISS data is only sensitive to the displacements of the Ag atoms relative to each other; the Ag-Si bonding geometry shown was constructed to be consistent with the interplaner distances reported by Takahashi [5] and our chemical intuition. However, Vlieg and van der Veen [13] and Ichimiya *et al.* [14] have presented convincing data that shows that the actual structure is not a simple silyl group termination as shown in the inset of Fig. 4, but probably involves a trimer of Si atoms below each Ag trimer. The agreement with the ICISS data for the trimer model is somewhat better than that for the honeycomb, although the honeycomb model cannot be completely ruled out based

on our data alone. The 180° backscattering ICISS data of Aono *et al.* [15] appears to distinguish more clearly between the honeycomb and trimer models, which suggests that ICISS data collected at different scattering angles can resolve ambiguities that may arise for a particular experimental orientation. At the present time, ICISS data collected along other azimuths and also with He ions as the projectile are being analyzed to better distinguish between the two different types of models for the Ag-induced reconstruction.

IV. Conclusions

The ICISS data for the Au- and Ag-induced reconstructions of Si(111) show conclusively that in both cases the metal atoms reside above the outermost Si layer, and that there are no Si adatoms above the metal atoms. For the Au covered surfaces, the ICISS data are consistent with primarily honeycomb and centered-hexagon models for the $\sqrt{3}\times\sqrt{3}$ and 6×6 surfaces, respectively, with the Au adatoms residing above the threefold-hollow sites. However, for the Ag-induced $\sqrt{3}\times\sqrt{3}$ surface, the data slightly favor a trimer arrangement of the Ag atoms, with a best fit yielding a Ag-Ag interatomic distance within the silyl group of 4.60 Å. This model is in close agreement with the models of Refs. [5,13-15] for the arrangement of the Ag atoms.

V. Acknowledgements

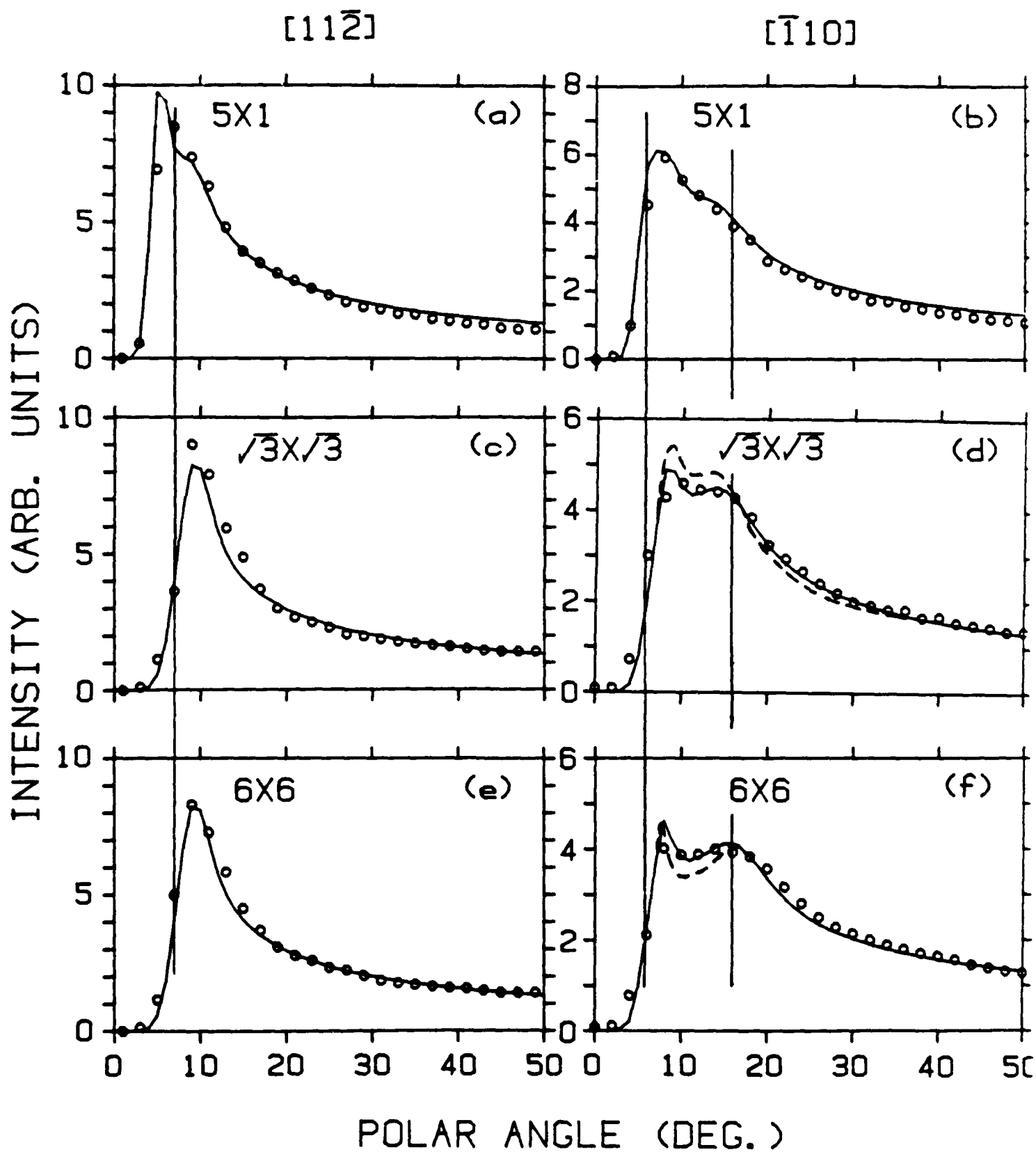
This research was supported by the National Science Foundation and the Camille and Henry Dreyfus Foundation. We thank M. Aono and M. Katayama for helpful discussions and for sharing their data prior to publication.

VI. References

- [1] G. Lelay, *Surf. Sci.* 132 (1983) 169.
- [2] S. Ino, *Jpn. J. Appl. Phys.* 16 (1977) 891.
- [3] E. J. van Loenen, J. E. Demuth, R. M. Tromp and R. J. Hamers, *Phys. Rev. Lett.* 58 (1987) 373.
- [4] R. J. Wilson and S. Chiang, *Phys. Rev. Lett.* 58 (1987) 369; *Phys. Rev. Lett.* 59 (1987) 2329.
- [5] T. Takahashi, S. Nakatani, N. Okamoto, T. Ishizawa, and S. Kikuta, *Jpn. J. Appl. Phys.* 27 (1988) L753.
- [6] Ph. Dumas, A. Humbert, G. Mathieu, P. Mathiez, C. Mouttet, R. Rolland, F. Savlan, and F. Thibaudau, *J. Vac. Sci. Technol.* A6 (1988) 517.
- [7] F. Salvan, private communication.
- [8] M. Aono, C. Oshima, S. Zaima, S. Otani and Y. Ishizawa, *Jpn. J. Appl. Phys.* 20 (1981) L829.
- [9] J. H. Huang and R. S. Williams, *J. Vac. Sci. Technol.* A6 (1988) 615; *Phys. Rev.* B38 (1988) 4022.
- [10] J. H. Huang and R. S. Williams, *Surf. Sci.* 204 (1988) 445.
- [11] R. S. Daley, J. H. Huang, and R. S. Williams, submitted to *Surf. Sci.*
- [12] A. Julg and A. Allouche, *Int. J. Quant. Chem.* 22 (1982) 739.
- [13] E. Vlieg and J. F. van der Veen, *Appl. Surf. Sci.* (this issue).
- [14] A. Ichimiya, S. Kohmoto, T. Fujii, and Y. Horio, *Appl. Surf. Sci.* (this issue).
- [15] M. Aono, M. Katayama, E. Nomura, and T. Soejima, *Appl. Surf. Sci.* (this issue).

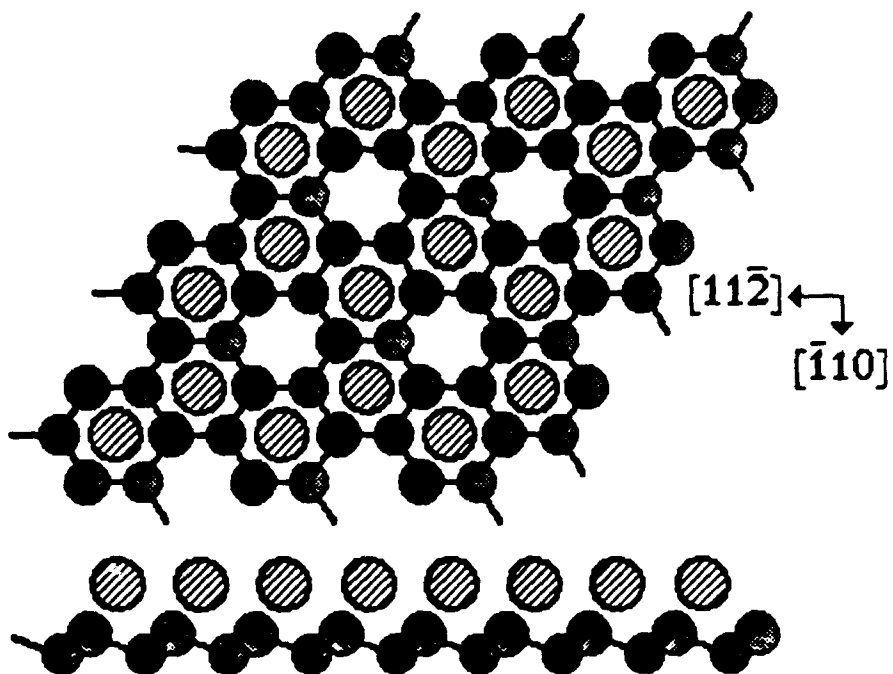
VII. Figure Captions

1. ICISS angular distributions (detected ion intensity as a function of the angle between the sample surface and the incident ion beam) for 5 keV Li ions scattered at 157° from Au atoms in the 5×1 , $\sqrt{3} \times \sqrt{3}$, and 6×6 reconstructions of Si(111) induced by Au overlayers. The distributions shown are for the $[11\bar{2}]$ and $[\bar{1}10]$ azimuths (the distributions along the $[\bar{1}\bar{1}2]$ and $[1\bar{1}0]$ azimuths, respectively, are essentially identical). The circles indicate the data points, and the lines are the result of calculations for the models described in the text.
2. Drawings of (a) a honeycomb overlayer on Si(111) in which the Au adatoms are located over the threefold-hollows, and (b.) a 6×6 unit cell on Si(111) based on a centered-hexagon array with 25% of the hexagons vacant. Slashed and dotted circles represent Au atoms, and darkly shades circles represent Si.
3. ICISS angular distributions for 5 keV Li ions scattered at 155° from the Ag-induced $\sqrt{3} \times \sqrt{3}$ reconstruction on Si(111). The experimental data (circles) were collected along the $[\bar{1}10]$ and the $[11\bar{2}]$ azimuths, but the scans along the $[1\bar{1}0]$ and $[\bar{1}\bar{1}2]$ azimuths, respectively, were essentially identical. Also shown are best fits (solid lines) to a trimer model in which the surface is terminated with (SiAg_3) groups (a, b), and a honeycomb model (c, d).
4. Drawing of the proposed trimer model for the Ag:Si(111)- $\sqrt{3} \times \sqrt{3}$ surface, with the inset showing the local bonding arrangement that was assumed. Slashed circles represent Ag atoms, and darkly shades circles represent Si.

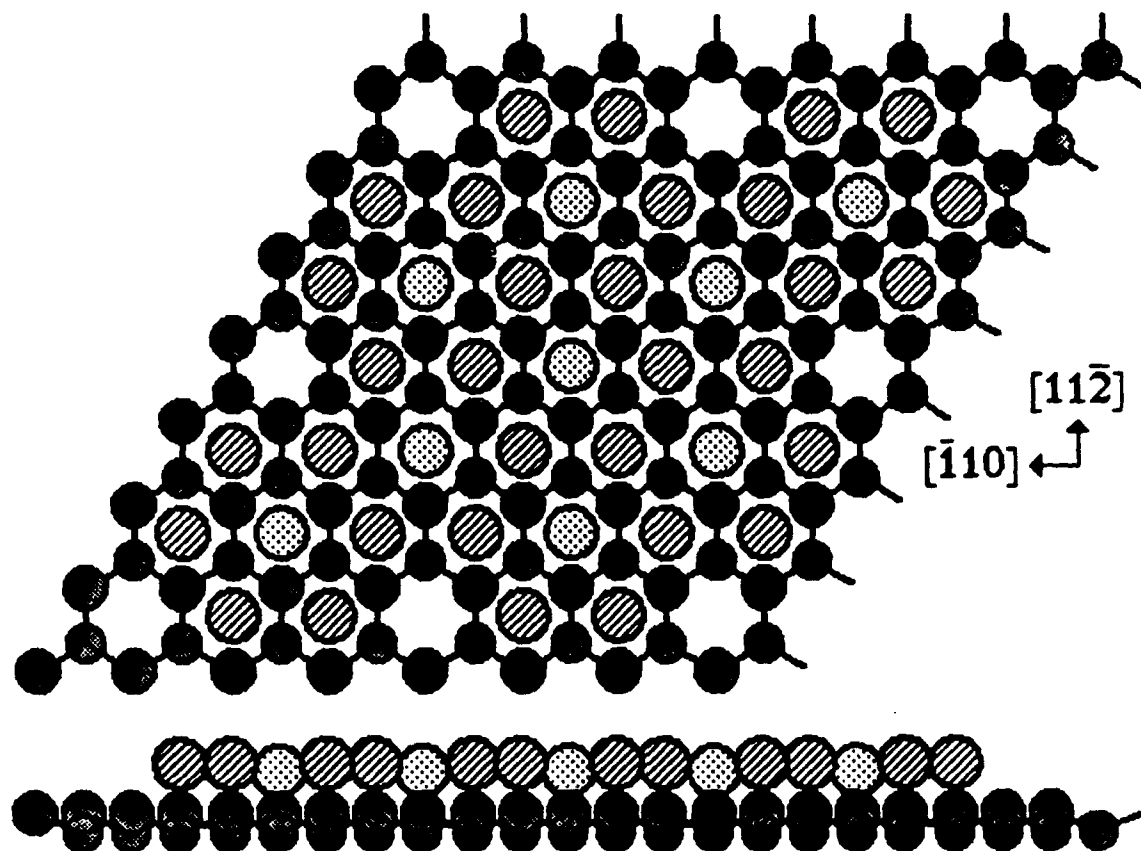


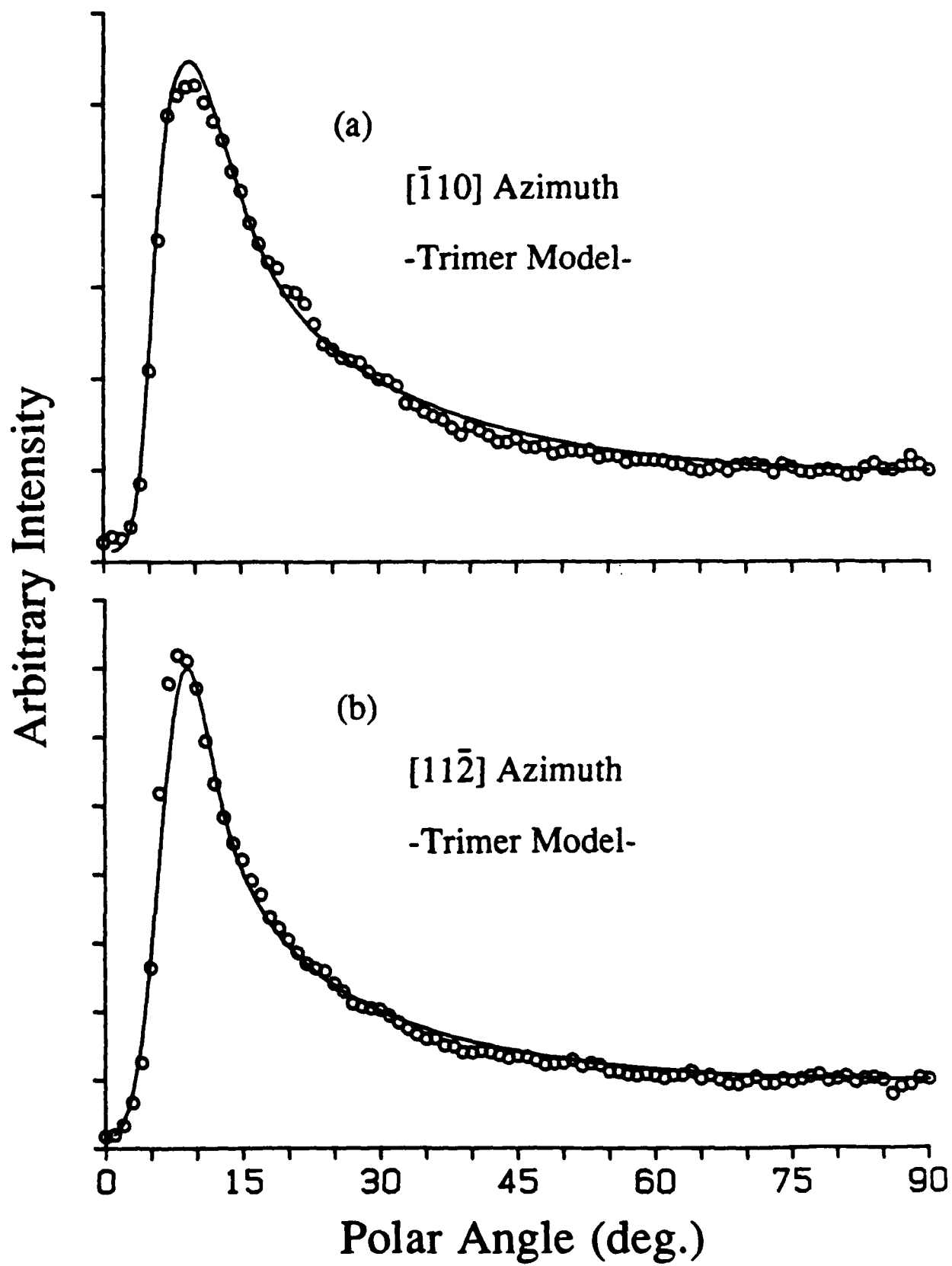
(a)

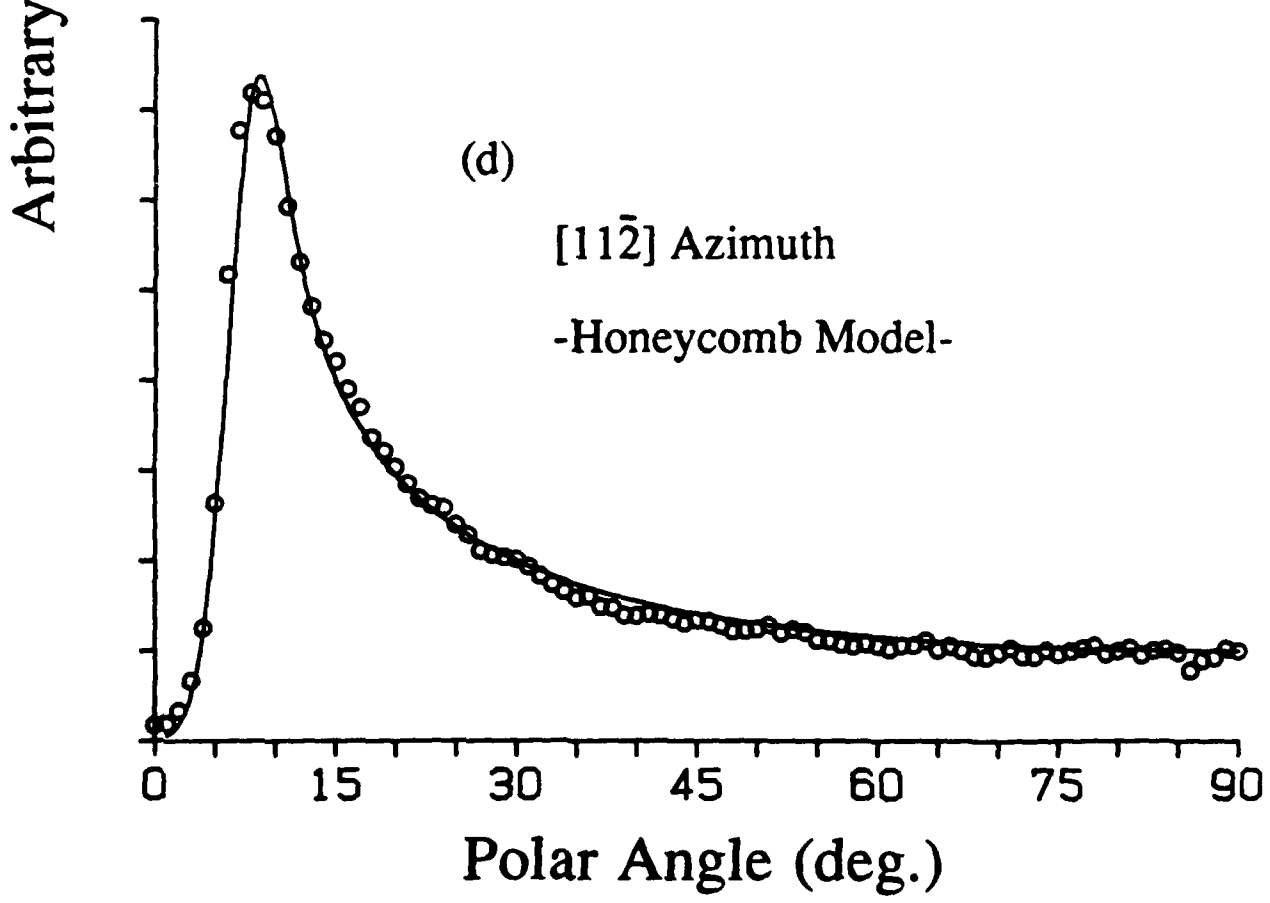
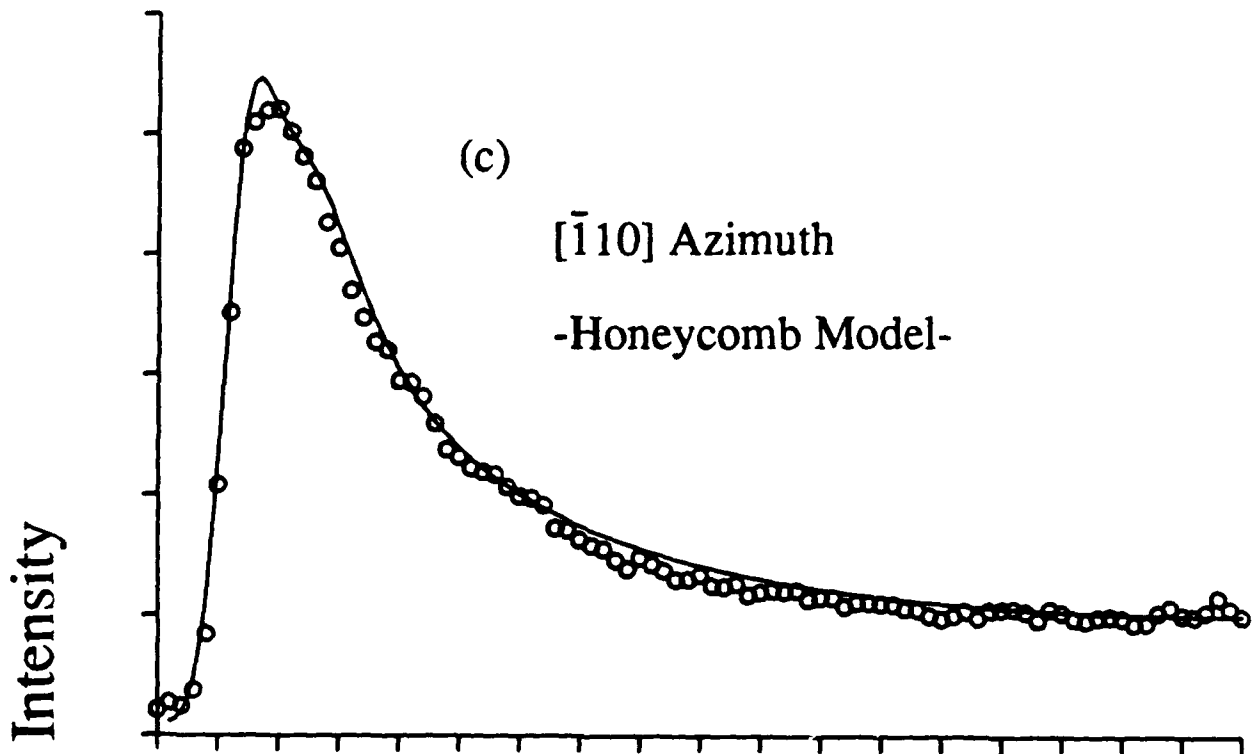
Model for Au- $\sqrt{3}\times\sqrt{3}$ Surface



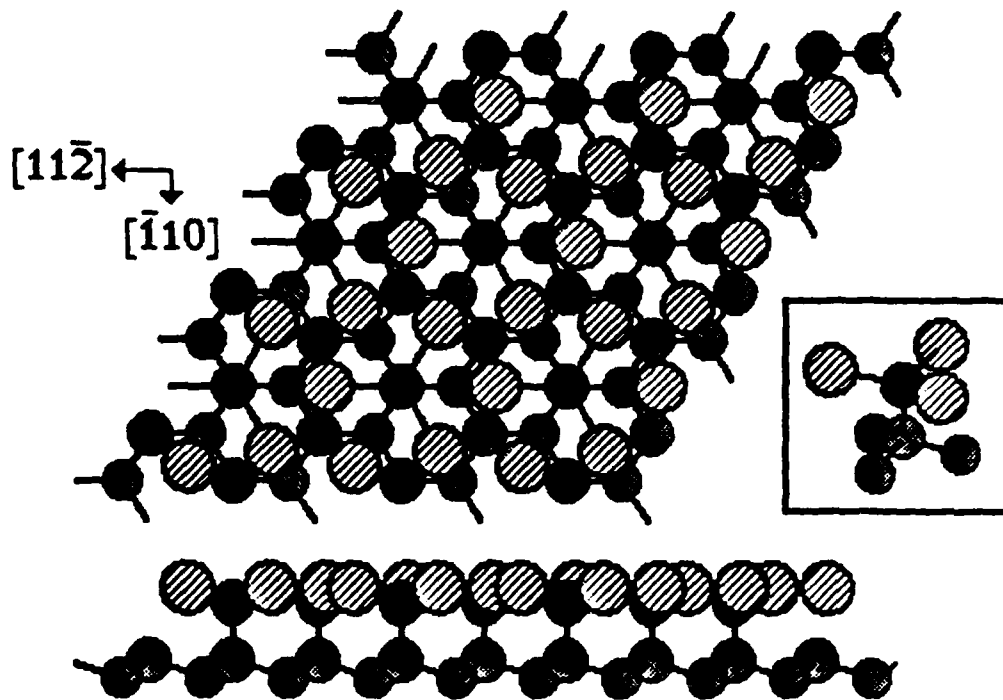
(b)
Model for Au-6x6 Surface







Proposed Model for Ag- $\sqrt{3}\times\sqrt{3}$ Surface



- Dr. J. Babbachwiler
Chemistry & Chem. Engrg.
Cull Inst. of Technology
Pasadena, CA 91125
- Dr. Paul G. Barbara
Department of Chemistry
University of Minnesota
Minneapolis, MN 55455-0431
- Dr. Duncan W. Brown
Adv. Technology Mails, Inc.
520-B Danbury Road
New Milford, CT 06776
- Dr. S. Bruchstein
Department of Chemistry
State University of NY
Buffalo, NY 14214
- Dr. J. Butler
Naval Research Laboratory
Code 6115
Washington, DC 20375-5000
- Dr. R.P.H. Chang
Mats. Science & Engineering
Northwestern University
Evanston, IL 60208
- Dr. Paul A. Christian
Adv. Chem. Technol., Fed. Systems
Eastman Kodak Company
Rochester, NY 14650-2156
- Dr. Richard Colton
Code 6170
Naval Research Laboratory
Washington, DC 20375-5000
- Dr. J.E. Deeneth
IBM Watson Research Center
PO Box 218
Yorktown Heights, NY 10598
- Dr. F.J. DiSalvo
Department of Chemistry
Cornell University
Ithaca, NY 14853
- Dr. A.B. Ellis
Department of Chemistry
University of Wisconsin
Madison, WI 53706
- Dr. M.A. El-Sayed
Chemistry Department
University of California
Los Angeles, 90024-1569
- Dr. John Eylez
Department of Chemistry
University of Florida
Gainesville, FL 32611
- Dr. James F. Garvey
Department of Chemistry
State University of New York
Buffalo, NY 14214
- Dr. T.F. George
Chemistry/Physics Depts.
State University of New York
Buffalo, NY 14260
- Dr. Arold Green
Quantum Surface Dynamics Br.
Naval Weapons Ctr.: Code 3817
China Lake, CA 93555
- Dr. R. Hamers
IBM Watson Research Center
PO Box 218
Yorktown Heights, NY 10598
- Dr. Paul K. Hansma
Department of Physics
University of California
Santa Barbara, CA 93106
- Dr. C.B. Harris
Chemistry Dept.
University of California
Berkeley, CA 94720
- Dr. J.C. Henzinger
Chemistry Dept.
University of California
Irvine, CA 92717
- Dr. Ronald Hoffmann
Chemistry Dept.
Cornell University
Ithaca, NY 14853
- Dr. L. Inerente
Chemistry Dept.
Rensselaer Polytech. Inst.
Troy, NY 12181
- Dr. E.A. Irene
Chemistry Dept.
Univ. of North Carolina
Chapel Hill, NC 27514
- Dr. D.E. Irish
Department of Chemistry
University of Waterloo
ONT N2L 3G1, Canada
- Dr. Mark Johnson
Department of Chemistry
Yale University
New Haven, CT 06511
- Dr. Sylvia M. Johnson
SRI International
333 Ravenswood Avenue
Menlo Park, CA 94025
- Dr. Z.H. Kafafi
Optical Sci. Div., Code 6551
Naval Research Laboratory
Washington, DC 20375-5000
- Dr. George H. Morrison
Chemistry Dept.
Cornell University
Ithaca, NY 14853
- Dr. Daniel M. Neumark
Chemistry Department
University of California
Berkeley, CA 94720
- Dr. D. Ramaker
Chemistry Dept.
George Washington Univ.
Washington, DC 20052
- Dr. R. Reeves
Chemistry Dept.
Rensselaer Polytech. Inst.
Troy, NY 12181
- Dr. A. Reisman
Microelectronics Center
Research Triangle Park
No. Carolina, 27709
- Dr. G. Rubloff
IBM Watson Research Ctr.
PO Box 218
Yorktown Hgts, NY 10598
- Dr. Richard J. Saykally
Chemistry Department
University of California
Berkeley, CA 94720
- Dr. Robert W. Shaw
US Army Research Office
Box 12211
Res. Triangle Park, NC 27709
- Dr. S. Sibener
James Franck Institute
University of Chicago
Chicago, IL 60637
- Dr. R.E. Smalley
Department of Chemistry
Rice University, Box 1892
Houston, TX 77251
- Dr. G.A. Somorjai
Chemistry Dept.
University of California
Berkeley, CA 94720
- Dr. G.B. Stringfellow
Mats. Science & Engineering
University of Utah
Salt Lake City, UT 84112
- Dr. Galen D. Stucky
Chemistry Dept.
University of California
Santa Barbara, CA 93106
- Dr. H. Tachikawa
Chemistry Dept.
Jackson State University
Jackson, MI 39217
- Dr. W. Uwertl
Surface Science & Technol. Lab
University of Maine
Orono, ME 04469
- Dr. R.P. Van Duynne
Chemistry Dept.
Northwestern University
Evanston, IL 60201
- Dr. David M. Walba
Chemistry Department
University of Colorado
Boulder, CO 80309-0215
- Dr. J.H. Weaver
Chemical Engrg & Mats. Sci.
University of Minnesota
Minneapolis, MN 55455
- Dr. B.R. Weiner
Department of Chemistry
University of Puerto Rico
Rio Piedras, PR 00931
- Dr. Robert L. Whetten
Chemistry Department
University of California
Los Angeles, CA 90024
- Dr. R. Stanley Williams
Dept. of Chemistry
University of California
Los Angeles, CA 90024
- Dr. N. Winograd
Chemistry Dept.
Case Western Res. Univ.
University Park, PA 16802
- Dr. A. Wold
Chemistry Dept.
Brown University
Providence, RI 02912
- Dr. John T. Yates
Chemistry Dept.
University of Pittsburgh
Pittsburgh, PA 15260
- Dr. E. Yeager
Chemistry Dept.
Case Western Reserve Univ.
Cleveland, OH 41106
- Dr. Richard W. Drisko
Naval Civil Engineering Lab
Code L-52
Port Huene, CA 93043
- Defense Tech. Information Ctr.
Building 5
Cameron Station
Alexandria, VA 22314
- David Taylor Research Center
Attn: Dr. Eugene C. Fischer
Applied Chemistry Division
Annapolis, MD 21402-5067
- Dr. James S. Munday
Chemistry Div., Code 6100
Naval Research Laboratory
Washington, DC 20375-5000
- Dr. David Nelson
Office of Naval Res. Code 413
800 N. Quincy Street
Arlington, VA 22217-5000
- Dr. Ronald L. Aitkins
Chemistry Div., Code 385
Naval Weapons Center
China Lake, CA 93555-6001
- Dr. Bernadette Eichinger
Naval Ships Systems Engr. Station
Phila. Naval Base, Code 053
Philadelphia, PA 19112
- David Taylor Research Station
Attn: Dr. H. H. Slingerman
Code 283
Annapolis, MD 21402-5067
- Dr. Sachio Yamamoto
Naval Ocean Systems Center
Code 52
San Diego, CA 91232
- Carlota Leufroy
Office of Naval Research
1030 E. Green Street
Pasadena, CA 91106
- Office of Naval Research
Spec. Assistant, Marine Corps
Code 00MC
800 N. Quincy Avenue
Arlington, VA 22217-5000
- Commanding Officer
Naval Weapons Support Center
Attn: Dr. Bernard E. Douada
Cran, IN 47522-5050